arXiv:1407.1161v3 [cond-mat.stat-mech] 1 Apr 2015

1D momentum-conserving systems: the conundrum of anomalous versus normal heat transport

Yunyun Li[1], Sha Liu[2], Nianbei Li[1*], Peter Hänggi[1,2,3,4], and Baowen Li[1,2,5]

[1] Center for Phononics and Thermal Energy Science, School of Physics Science and Engineering, Tongji University, 200092 Shanghai, China
[2] Department of Physics and Centre for Computational Science and Engineering, National University of Singapore, 117456, Singapore
[3] Institut für Physik, Universität Augsburg, Universitätsstr. 1, 86159 Augsburg, Germany
[4] Nanosystems Initiative Munich, Schellingstr, 4, D-80799 München, Germany
[5] Center for Computational Science and Engineering, Graphene Research Centre, Department of Physics, National University of Singapore, 117456 Singapore

E-mail: nbli@tongji.edu.cn

Abstract.

Transport and the spread of heat in Hamiltonian one dimensional (1D) momentum conserving nonlinear systems is commonly thought to proceed anomalously. Notable exceptions, however, do exist of which the coupled rotator model is a prominent case. Therefore, the quest arises to identify the origin of manifest anomalous energy and momentum transport in those low dimensional systems. We develop the theory for both, the statistical densities for momentum- and energy-spread and particularly its momentum-/heat-diffusion behavior, as well as its corresponding momentum/heat transport features. We demonstrate that the second temporal derivative of the mean squared deviation of the momentum spread is proportional to the equilibrium correlation of the total momentum flux. Subtracting the part which corresponds to a ballistic momentum spread relates (via this integrated, subleading momentum flux correlation) to an effective viscosity, or equivalently, to the underlying momentum diffusivity. We next put forward the intriguing hypothesis: normal spread of this so adjusted excess momentum density causes normal energy spread and alike normal heat transport (Fourier Law). Its corollary being that an anomalous, superdiffusive broadening of this adjusted excess momentum density in turn implies an anomalous energy spread and correspondingly anomalous, superdiffusive heat transport. This hypothesis is successfully corroborated within extensive molecular dynamics simulations over large extended time scales. Our numerical validation of the hypothesis involves four distinct archetype classes of nonlinear pair-interaction potentials: (i) a globally bounded pair interaction (the noted coupled rotator model), (ii) unbounded interactions acting at large distances (the coupled rotator model amended with harmonic pair interactions), (iii) the case of a hard point gas with unbounded square well interactions and (iv) a pair interaction potential being unbounded at short distances while displaying an asymptotic free part (Lennard-Jones model). We compare our findings with recent predictions obtained from nonlinear fluctuating hydrodynamics theory.

1. Introduction

The investigation of heat conduction in low dimensional nonlinear lattices has attracted ever increasing attention in the statistical physics community [1, 2, 3]. Although early relevant work [4] can be traced back to 1993, an increased activity has spurred since the discovery of anomalous heat conduction occurring in one dimensional (1D) momentum-conserving Fermi-Pasta-Ulam (FPU)-β lattices [5] in 1997. In those low dimensional study cases the thermal conductivity κ of the FPU-β lattice was found to diverge with the lattice size N as $\kappa \propto N^{\alpha}$, with $0 < \alpha < 1$. This finding consequently yields a system-size dependent thermal conductivity, thus breaking Fourier's law of heat conduction. Similar anomalous heat conduction behavior has also been identified for other archetype 1D momentum-conserving stylized nonlinear systems, such as the 1D diatomic Toda lattices [6], and, importantly, has been predicted to occur in momentum-conserving physical materials, such as in carbon nanotubes [7], silicon nanowires [8] and in polymer chains [9]. Experimentally, the breakdown of Fourier's law has presently been confirmed for 1D carbon nanotubes and boron-nitride nanotubes [10] and in 2D suspended graphene [11].

On the other hand, the low (1D, 2D) spatial dimension alone is not the sole feature that determines whether the validity of Fourier's law holds up. For example, normal heat conduction obeying Fourier's law has been established beyond doubt for 1D nonlinear Frenkel-Kontorova (FK) [12] lattices and ϕ^4 lattices [13, 14]. For those nonlinear lattice systems the total momentum is not conserved, being due to the presence of the on-site potentials. These numerical results for 1D lattices led to a conjecture that the property of momentum-conservation in low dimensional systems might be at the origin to give rise to anomalous heat conduction for 1D and 2D nonlinear lattices, e.g. see [1, 2, 15, 16]. It then later came as a surprise that contradictory results emerged for other stylized momentum-conserved nonlinear 1D lattices, exhibiting saturated thermal conductivities such as the rotator model [17, 18] and a momentum-conserving variation of the ding-a-ling model [19]. Giardinà and Kurchan also provided a family of models with or without momentum-conservation which, however, all obey Fourier's law [20]. Therefore this situation gives rise to the dilemma of what physics is at the root for the occurrence of the breakdown of the Fourier behavior in 1D nonlinear lattices [21, 22]. Most recently, relying on numerical simulations, Savin and Kosevich [23] showed that thermal conduction obeys Fourier's law for 1D momentum-conserving lattices with a 1D Lennard-Jones interaction, a Morse interaction, and as well a Coulomb-like interaction. Those numerical findings let them to conclude (we think erroneously, see in Sect. 4.4 below, and, as well, in Ref. [24]) that normal heat conduction emerges for momentum-conserving lattices whenever the pair interaction potentials are asymptotically free at large interaction distances.

In this work, we focus on heat transport in 1D momentum-conserving nonlinear lattices from another aspect, namely, the *diffusive spread* of energy and momentum. It is acknowledged that there exists a profound connection between heat conduction and

heat diffusion within the region where Fourier's law is valid. For example, take the normal heat conduction in 1D cases: Fourier's law states that $j = -\kappa\partial_x T$, where j denotes the local heat flux and $\partial_x T$ is the nonequilibrium temperature gradient. If we combine this with local energy conservation; i.e., $\partial_t E + \partial_x j = 0$ and, additionally, use the relation between the local energy density E and the temperature T, i.e., $E = c_{\rm V} T$ (with $c_{\rm V}$ being the volumetric specific heat), then the familiar heat diffusion equation $\partial_t T = D\partial_x^2 T$ can be derived. The normal heat diffusivity equals $D = \kappa/c_{\rm V}$.

Microscopically, normal heat diffusion can be characterized by the mean square displacement of the corresponding Helfand moment [25], which then connects to normal heat conductivity via the Green-Kubo formula. The efforts trying to bridge heat conduction and diffusion beyond the normal case have only been put forward in the recent decade [22, 24, 26, 27, 28, 29, 30, 31, 32, 33]. Remarkably, it is only recently that a general and rigorous connection between heat conduction and heat diffusion has been established from first principles [34]: It is shown that in the linear response regime, the evolution of the second order time-derivative of the mean squared deviation (MSD) of a general energy diffusion process is determined by the equilibrium heat flux autocorrelation function of the system – the central quantity that enters the Green-Kubo formula for the thermal heat conductivity. The key ingredient for obtaining this MSD of the energy spread relies on the energy-energy correlation function $C_E(x,t;x',0)$ [35], as rigorously shown in recent work [34]. This thermal equilibrium excess energy-energy correlation indeed is the fundamental quantity that determines the behavior of nonequilibrium heat diffusion, as well as the nonequilibrium heat conduction in a regime not too far displaced from thermal equilibrium. Thus, using the energy-energy correlation function, we can conveniently identify whether the heat diffusion in a nonlinear lattice occurs normal or anomalous.

With this present study we aim to shed more light on the conundrum that underpins anomalous heat transport in 1D nonlinear lattices. In doing so we study with molecular dynamics (MD) simulations four different nonlinear 1D momentum-conserving nonlinear lattices. The 1-st one is the 1D coupled rotator lattice which has a bounded interaction potential; i.e., the potential is bounded in configuration space and therefore the motion of the particles are not confined. The 2-nd test case studies an unbounded harmonic interaction potential in combination with the coupled rotator interaction potential. The 3-rd test case is the hard point gas model with alternating masses subject to infinite square well pair interactions. This model is believed to show good mixing properties and therefore fast convergence features. As yet a 4-th 1D nonlinear system we complement the rotator model with a Lennard-Jones 1D-interaction potential, being unbounded at short interaction distances while being free at large interaction distances. This latter model thus allows for bond dissociation at large interaction distances. For all these test beds the correlation functions for the local excess energy deviations as well as the local excess momentum are calculated via extensive equilibrium numerical MD-simulations.

Our studies corroborate the result that normal heat diffusion is found for the coupled rotator lattice. We also demonstrate that in addition to normal heat diffusion

the overall dynamics is accompanied by a normal momentum diffusion. We then elucidate that these two features imply that the system dynamics is ruled by the emergence of a finite momentum diffusivity. This observation therefore insinuates that the 1D rotator model physically mimics a fluid behavior. In clear contrast, we find that anomalous heat diffusion occurs for momentum-conserving nonlinear 1D lattices which contain an unbounded interaction potential, as it is the case also with nonlinear FPU-lattices, the hard point gas and also the Lennard-Jones case. The anomalous heat diffusion and corresponding anomalous heat conductivity behavior is shown to be accompanied in all those test cases with the momentum excess density to undergo anomalous superdiffusion. This latter feature causes a divergent effective viscosity, thus mimicking physically a solid-like behavior.

The present study is organized as follows. In Section 2, we briefly review the state of the art of the theory for excess energy diffusion and then develop the theory describing the diffusion of excess momentum. In Section 3, we put forward our hypothesis for the occurrence of normal/anomalous heat transport. This hypothesis is tested thoroughly in Section 4. We start out by performing numerical studies on an overall bounded interaction potential, namely the coupled rotator model. This is then followed by studying a variant of this rotator model by complementing it with unbounded harmonic pair interactions. In addition we discuss the cases with a hard point gas and a Lennard-Jones pair interaction. These detailed numerical MD studies for these four nonlinear lattice systems support the fact that it is not the mere presence or absence of the symmetry of momentum conservation but rather the presence or absence of a fluid-like behavior, as characterized with normal spread of the momentum excess density, which we speculate to be at the source for the validity or the breakdown of Fourier's law behavior. For the prior known cases with the dynamics subjected in addition to nonlinear on-site potentials the momentum conservation is broken: the emergence of Fourier's Law in this latter situation is then ruled by nonlinear scattering processes which provide a finite mean free path behavior for the heat transfer [36]. Additional conclusions and remaining open issues are presented with Section 5.

2. Diffusion of heat and momentum

Let us consider systems with a momentum-conserving, homogeneous 1D nonlinear Hamiltonian lattice dynamics with nearest neighbor interactions. Their Hamiltonian can be cast in the general form

$$H = \sum_i \left[\frac{p_i^2}{2m} + V(q_{i+1} - q_i) \right] \equiv \sum_i H_i \ , \tag{1}$$

where the set p_i denote the momenta of particles of identical masses m. The set q_i are the displacements from the equilibrium position for the i-th atom with $i = 0, \pm 1, \pm 2, ..., \pm(N-1)/2$, where an odd value of N is assumed for the sake of convenience. The part $V(q_{i+1} - q_i)$ is the interaction potential between neighboring sites i and $i+1$. With H_i we formally denote the local energy at site i. Moreover, throughout

our numerical analysis we shall make use of periodic boundary conditions; i.e., we set $q_{N+i} = q_i$ and $p_{N+i} = p_i$. The center of mass velocity of the system is chosen at rest; i.e. $v_{cm} = 0$. Note also that we use here strictly Hamiltonian lattice systems which contain no stochastic interaction parts of a spatial or a temporal nature.

2.1. Heat diffusion

We start out with the description of heat diffusion in a discrete 1D lattice following Ref. [34]. In doing so, we introduce the energy-energy correlation function, reading:

$$C_E(i,t;j,0) \equiv \frac{\langle \Delta H_i(t) \Delta H_j(0) \rangle}{k_B T^2 c_{\rm V}}, \tag{2}$$

where $\Delta H_i(t) \equiv H_i(t) - \langle H_i(t) \rangle$ and $\langle \cdots \rangle$ denotes the ensemble average over canonical thermal equilibrium at a temperature T and $c_{\rm V}$ is the specific heat per particle.

Given this autocorrelation function of energy fluctuations, one can evaluate the time evolution of the excess energy distribution $\rho_E(i,t)$ starting out from an initial, near thermal equilibrium state, characterized by the initial excess energy perturbation $\xi(i)$. We consider the case of a localized, small initial excess energy perturbation at the central site, i.e., $\xi(i) = \epsilon \delta_{i,0}$. We can then use linear response theory for the excess energy distribution $\rho_E(i,t)$ to obtain [34]:

$$\rho_E(i,t) = \sum_j C_E(i,t;j,0)\xi(j)/\epsilon = C_E(i,t;j=0,t=0), \ -\frac{N-1}{2} \leq i \leq \frac{N-1}{2}. \tag{3}$$

This excess energy distribution remains normalized at all later times t, being due to the conservation of energy.

The commonly used quantity which quantifies the speed of *heat diffusion* is the MSD $\langle \Delta x^2(t) \rangle_E$ of the excess energy distribution. For a discrete 1D lattice with N sites one thus obtains with $\langle x(t) \rangle_E = 0$

$$\left\langle \Delta x^2(t) \right\rangle_E \equiv \sum_i i^2 \rho_E(i,t) = \sum_i i^2 C_E(i,t;j=0,t=0), \ -\frac{N-1}{2} \leq i \leq \frac{N-1}{2}, \tag{4}$$

This MSD has been shown to obey the salient second order differential equation [34]; i.e.,

$$\frac{d^2 \langle \Delta x^2(t) \rangle_E}{dt^2} = \frac{2}{k_B T^2 c_{\rm V}} C_J(t) \ , \tag{5}$$

where $C_J(t)$ denotes the equilibrium autocorrelation function of total heat flux defined as

$$C_J(t) = \frac{1}{N} \langle \Delta J(t) \Delta J(0) \rangle \ , \ J(t) = \sum_i j_i \ , \tag{6}$$

wherein $j_i \equiv -\frac{p_i}{m} \partial V(q_i - q_{i-1})/\partial q_i$ is the local heat flux. Note that this correlation $C_J(t)$ is just what enters the Green-Kubo formula for thermal conductivity [1, 2, 37, 38], being written as $\langle J(t) J(0) \rangle / N$. This is so because here with $v_{cm} = 0$ and $\Delta J(t) = J(t)$, as the equilibrium average obeys $\langle J(t) \rangle = 0$. Moreover, $J(t)$ contains no energy current

stemming from transporting charge in an electromagnetic field or an energy current stemming from a particle concentration gradient.

$C_J(t)$ is the quantity that enters the well-known Green-Kubo expression for the thermal conductivity κ. For normal heat flow it explicitly reads, $\kappa = 1/(k_B T^2)\int_0^\infty C_J(t)dt$.

The relation in (5) connects heat conduction with heat diffusion in a rigorous way. As a consequence, the investigation of heat conduction can equivalently be obtained from studying heat diffusion. The most important quantity is the energy fluctuation autocorrelation function $C_E(i,t;j=0,t=0)$ in Eq. (2); it encodes all the necessary information about heat diffusion and heat conduction. As one can defer from Eq. (4) and Eq. (5), the energy-energy correlation function $C_E(i,t;j=0,t=0)$ determines the dynamical behavior of the MSD of heat diffusion as well as the autocorrelation function of total heat flux $C_J(t)$.

As an example take the FPU-β model which displays anomalous heat diffusion: there, the energy autocorrelation $C_E(i,t;j=0,t=0)$ follows a Levy walk distribution, being quite distinct from a normal Gaussian distribution in the long time limit [27, 28, 35]. This statistics then gives rise to a superdiffusive behavior for the energy spread, reading

$$\left\langle \Delta x^2(t)\right\rangle_E \sim t^\beta,\ 1<\beta<2\ . \tag{7}$$

The corresponding, formally diverging anomalous thermal conductivity can be extracted to read [34]

$$\kappa \sim \frac{1}{k_B T^2}\int_0^{N/c} C_J(t)dt = \frac{c_{\rm V}}{2}\frac{d\left\langle \Delta x^2(t)\right\rangle_E}{dt}\bigg|_{t\sim N/c} \propto N^{\beta-1}\ . \tag{8}$$

Here, $t_s \sim N/c$ with N chosen sufficiently large presents the characteristic time-scale of heat diffusion. The quantity c refers to the speed of sound for inherent renormalized phonons [39].

2.2. Momentum diffusion

The scheme for the excess energy heat diffusion can likewise be generalized for the problem of corresponding diffusion of excess momentum. For a nonlinear lattices with a Hamiltonian in Eq. (1), the translational invariance of the Hamiltonian necessarily indicates that the total momentum $\sum_i p_i$ is conserved; i.e., we have

$$\frac{d\sum_i p_i}{dt} = -\sum_i\left(\frac{\partial V(q_i-q_{i-1})}{\partial q_i} - \frac{\partial V(q_{i+1}-q_i)}{\partial q_{i+1}}\right) = 0\ , \tag{9}$$

by observing that $\partial V(q_{i+1}-q_i)/\partial q_i = -\partial V(q_{i+1}-q_i)/\partial q_{i+1}$.

Using an analogous reasoning as put forward with the preceding subsection for heat diffusion we can define the autocorrelation function for the excess momentum fluctuation [35], reading explicitly:

$$C_P(i,t;j,0) = \frac{\langle \Delta p_i(t)\Delta p_j(0)\rangle}{mk_BT}, \tag{10}$$

where $\Delta p_i(t) \equiv p_i(t) - \langle p_i(t)\rangle = p_i(t)$, observing that $\langle p_i(t)\rangle = 0$ in thermal equilibrium. Following the reasoning of the previous subsection we next demonstrate that this momentum-momentum autocorrelation function describes, within linear response theory, the diffusion of momentum along the lattice.

To elucidate this issue we consider alike a lattice in thermal equilibrium at temperature T. We apply a small kick of short duration to the j-th particle. The kick occurs with a constant impulse $\mathcal{I}$, yielding a force kick at site j as

$$f_j(t) = \mathcal{I}\delta(t). \tag{11}$$

Upon integrating the equation of motion from the moment immediately before the kick (denoted as $t = 0^-$) to the moment immediately after the kick (denoted as $t = 0^+$), we find that the sole effect of this kick is to change the momentum of the jth particle by an amount $\mathcal{I}$. The momenta of all other particles, as well as the position of all particles remain unchanged. Formally, this is recast as

$$p_i(t = 0^+) - p_i(t = 0^-) = \mathcal{I}\delta_{i,j}; \tag{12}$$

$$q_i(t = 0^+) - q_i(t = 0^-) = 0. \tag{13}$$

The full time evolution of the momenta and positions is not analytically accessible for non-integrable nonlinear lattice systems. However, given that $\mathcal{I}$ is small, the validity regime of linear response is obeyed. The explicit response can be obtained by referring to canonical linear response theory for an isolated system [40]. Specifically, we assume that the system has been prepared in the infinite past, $t = -\infty$, with the canonical distribution

$$\rho(t = -\infty) = \rho_{eq} = \frac{1}{Z}\exp[-\beta_T H]; \quad Z = \int d\Gamma \exp[-\beta_T H]\ , \tag{14}$$

where $\beta_T = 1/k_B T$ and $d\Gamma = dq_1 \cdots dp_1 \cdots$. With a time dependent force $f_j(t)$ applied to the jth particle, the total Hamiltonian reads $H_{tot} = H - f_j(t)q_j$. With the system dynamics being closed, the evolution of the phase space distribution is governed by the Liouville equation

$$\frac{\partial \rho(t)}{\partial t} = \{H_{tot}, \rho(t)\} \equiv L_{tot}\rho(t)\ , \tag{15}$$

where $\{\cdots, \cdots\}$ denotes the Poisson bracket. The linear response solution can be readily obtained up to the first order of f_j, yielding

$$\rho(t) = \rho_{eq} + \Delta\rho(t) = \rho_{eq} + \frac{1}{mk_B T}\int_0^\infty ds e^{Ls} p_j \rho_{eq} f_j(t - s), \tag{16}$$

The operator L is the Liouville operator for the original, unperturbed system, i.e. $LA = \{H, A\}$ for any quantity A. Therefore, in presence of the kick-force the thermally averaged particle momenta read for $t > 0$

$$\langle p_i(t)\rangle_{response} = \int p_i \Delta\rho(t) d\Gamma = \frac{\mathcal{I}\,\langle \Delta p_i(t)\Delta p_j(0)\rangle}{mk_B T} = \mathcal{I}C_P(i, t; j, 0). \tag{17}$$

For $t = 0^+$, it reduces to $\langle p_i(0^+)\rangle_{response} = \mathcal{I}\delta_{i,j}$ due to equipartition $\langle p_i(0)p_j(0)\rangle = mk_B T\delta_{i,j}$, which is consistent with Eq. (12).

The conservation of total momentum implies that, $\sum_i \langle p_i(t)\rangle_{response}$, is conserved as well. Evaluating this sum at time $t = 0$ yields $\sum_i C_P(i,t;j,0) = 1$ for all later times t. The excess momentum density function $\rho_P(i,t)$ therefore assumes the form

$$\rho_P(i,t) = \frac{\langle p_i(t)\rangle_{response}}{\sum_i \langle p_i(t)\rangle_{response}} = C_P(i,t;j,0), \tag{18}$$

which remains normalized in the course of time $t > 0$. The density $\rho_P(i,t)$ is, however, not necessarily semi-positive everywhere; i.e. it again does not present a manifest probability density for all later times t.

With time evolving, we notice that the excess momentum autocorrelation Eq. (10) describes the spread of the momentum distribution after the initial kick has occurred. As can be observed below, for increasing times t the quantity $C_P(j,t;j,0)$ decreases (at least for some finite time). This implies the decrease of the momentum of the j'th particle. The lost momentum is transferred to its neighbors. This feature physically mimics a viscous behavior.

Let us next assume that the kick is applied to the center particle; i.e. we explicitly set $j = 0$. Similarly to Eq. (4), we define the MSD of the excess *momentum* $\langle \Delta x^2(t)\rangle_P$ for a discrete lattice as

$$\left\langle \Delta x^2(t)\right\rangle_P = \sum_i i^2 \rho_P(i,t) = \sum_i i^2 C_P(i,t;j=0,t=0),\ -\frac{N-1}{2} \le i \le \frac{N-1}{2}\ . \tag{19}$$

Because of the conservation of total momentum, in analogy to the energy continuity relation, we may define a "momentum flux" j_i^P via the local momentum continuity relation. To see this, we write down the Newtonian equation of motion for the i'th particle, reading

$$\frac{dp_i}{dt} = -\frac{\partial V(q_i - q_{i-1})}{\partial q_i} - \frac{\partial V(q_{i+1} - q_i)}{\partial q_i}. \tag{20}$$

By defining the momentum flux as $j_i^P = -\partial V(q_i - q_{i-1})/\partial q_i = \partial V(q_i - q_{i-1})/\partial q_{i-1}$, we obtain a discrete form of the momentum continuity relation, reading

$$\frac{dp_i}{dt} - j_i^P + j_{i+1}^P = 0\ . \tag{21}$$

Note that the momentum flux j_i^P is actually the force exerted on particle i from particle $(i-1)$. Its ensemble average $\left\langle j_i^P\right\rangle$ yields the average internal pressure.

Following the strategy used for heat diffusion, one can derive a corresponding relation for the second time derivative $\langle \Delta x^2(t)\rangle_P$. It reads:

$$\frac{d^2\langle \Delta x^2(t)\rangle_P}{dt^2} = \frac{2}{mk_BT} C_{J^P}(t)\ . \tag{22}$$

Here, the centered autocorrelation function of the momentum flux is given by

$$C_{J^P}(t) = \frac{1}{N}\left\langle \Delta J^P(t)\Delta J^P(0)\right\rangle,\ J^P = \sum_i j_i^P\ . \tag{23}$$

It should be observed that here the momentum flux $\Delta J^P(t)$, unlike for energy flux, cannot be replaced with $J^P(t)$ itself. This is so because the equilibrium average is

typically non-vanishing with $\left\langle J^P(t)\right\rangle = N\Lambda$, where Λ denotes a possibly non-vanishing internal equilibrium pressure in cases where the interaction potential is not symmetric.

The presence of a finite, isothermal sound speed c may imply that the momentum spread contains a ballistic component. Spreading then occurs into the positive and negative directions with velocity c, with the two centers of equal weight $1/2$ moving at velocities $\pm c$ [25]. We hence must subtract this trivial ballistic part $\frac{1}{2}c^2t^2$ for the weighted $(\frac{1}{2})$ one-sided spread in configuration space. The effective bulk viscosity η is thus given as an integration over this *subleading* excess momentum correlation $C_{J^P}(t)$ over time in terms of a Green-Kubo formula [25, 41], reading

$$\eta \equiv \lim_{t\to\infty}\Big(\frac{1}{k_BT}\int_0^t C_{J^P}(t)dt - \frac{1}{2}mc^2t\Big). \tag{24}$$

In case that the momentum diffusion occurs normal one can invoke the concept of a finite momentum diffusivity by defining, upon use of eqs. (22, 24):

$$2D_P \equiv \lim_{t\to\infty}\Big(\frac{d\left\langle\Delta x^2(t)\right\rangle_P}{dt} - c^2t\Big)\ . \tag{25}$$

Therefore, for the discrete lattices discussed here, this so introduced viscosity η precisely equals the momentum diffusivity times the atom mass, namely

$$\eta = mD_P\ . \tag{26}$$

Given a situation where the excess momentum density spreads not normally the limit in Eq. (25) no longer exits. The integration in Eq. (24) formally diverges, thus leading to an infinite viscosity.

In the context of this work we find that such an infinite viscosity indicates a manifest solid-like behavior. In distinct contrast, however, a result with a finite effective viscosity indicates an effective fluid-like behavior.

3. The hypothesis

The general folklore in the field of anomalous heat conduction [15, 16] is that in momentum-conserving 1D nonlinear lattices one encounters an anomalous heat conductance behavior. The case with the rotator model, however, presents an eminent exception. So what is the physical mechanism which can explain such exceptions? – An observation is that in all those presently known cases exhibiting anomalous 1D heat conductance the interaction potential has been of unbounded nature at large interaction distances. The known exceptions, predominantly the well studied case with the rotator model, do not possess such unbounded pair interactions at long distances. Obviously the form of the overall interaction does matter for the violation of Fourier's law. One may speculate that the emergence of the anomalous behavior is rooted in the form of an excess momentum density dynamics that behaves solid-like in the sense that the momentum diffusion does not support a finite effective viscosity in the spirit defined above. In contrast, a Fourier-like behavior may become possible if the inherent momentum dynamics is more fluid-like, consequently possessing a finite effective momentum

diffusivity. An appealing conjecture therefore is that it is the physics of momentum diffusion which rules whether heat transport occurs normal or anomalous. In short, we next test with different models the following hypothesis:

(i) *Heat transport in nonlinear 1D momentum-conserving Hamiltonian lattice systems occurs normal whenever the spread of the profile of the excess momentum density, upon subtracting a possibly present leading ballistic part, is normal.*

(ii) *The corollary being that heat transport occurs anomalous whenever this so adjusted, subleading momentum excess density spreads superdiffusive.*

If this hypothesis holds true it is expected to hold vice versa, i.e., with heat/momentum substituted by momentum/energy.

4. Testing the hypothesis

We next test this so stated hypothesis numerically with four classes of nonlinear Hamiltonian lattice dynamics. The numerical procedure used and the details of scaling of parameters and dimensionless units are deferred to the Appendix.

4.1. Coupled rotator dynamics

As a first test bed for the above hypothesis we scrutinize the normal heat transport behavior in a nonlinear, momentum-conserving 1D occurring with the coupled rotator lattice. Throughout the remaining we shall use Hamiltonian lattice models with corresponding dimensionless units [1, 2]. The Hamiltonian for the coupled rotator lattice dynamics reads

$$H = \sum_i \Big(\frac{p_i^2}{2} + [1 - \cos(q_{i+1} - q_i)] \Big) \, . \tag{27}$$

Notably, here the nonlinear, momentum-conserving interaction potential is bounded for all arguments via the cosine function. The local energy density is $H_i = p_i^2/2 + [1 - \cos(q_{i+1} - q_i)]$. Without loss of generality, we consider the initial distribution of the excess energy or momentum to be a Kronecker-delta function in the lattice center. The autocorrelation functions $C_E(i, t; j = 0, t = 0)$ and $C_P(i, t; j = 0, t = 0)$ for energy and momentum are defined according to Eqs. (2) and (10). Thus, the temporo-spatial behavior of $C_E(i, t; j = 0, t = 0)$ and $C_P(i, t; j = 0, t = 0)$ describe the dynamics of energy and momentum diffusion starting out from the central position. With the interaction potential being symmetric there is vanishing internal pressure.

In Fig. 1 (a), we depict the correlation functions $C_E(i, t; j = 0, t = 0)$ for the energy diffusion versus evolving relative time span t. For sufficiently large times t we observe that the energy autocorrelation function $C_E(i, t; j = 0, t = 0)$ evolves very closely into

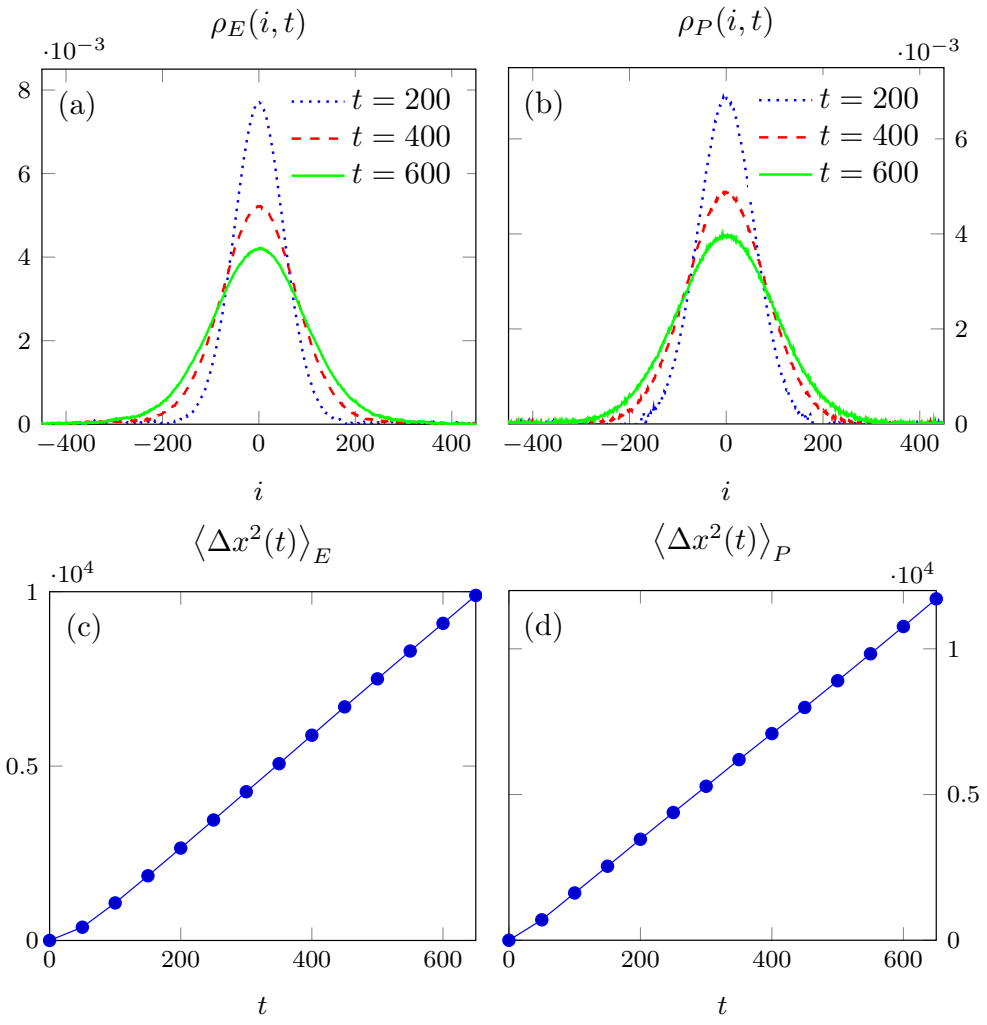

Figure 1. (color online) Heat and momentum transport in the coupled rotator model: Upper panels (a) and (b): Spatial distribution of the energy autocorrelation $\rho_E(i,t) = C_E(i,t;j=0,t=0)$ and the momentum autocorrelation $\rho_P(i,t) = C_P(i,t;j=0,t=0)$, respectively. The correlation times are $t = 200$ (dotted blue), 400 (dashed red), and 600 (solid green). Lower panels (c) and (d): The mean squared deviation (MSD) of the energy $\langle \Delta x^2(t) \rangle_E$ and the momentum $\langle \Delta x^2(t) \rangle_P$, respectively. A perfect linear time dependence of the MSD can be clearly detected for both, the energy and the momentum. The lattice size is chosen $N = 1501$ and the temperature is $T \approx 0.413$.

a Gaussian distribution function (but still spatially bounded with the causal cone, as determined by a finite speed of sound); i.e., its profile is perfectly well given by

$$C_E(i,t) \sim \frac{1}{\sqrt{4\pi D_E t}} e^{-\frac{i^2}{4D_E t}} \tag{28}$$

with D_E denoting the diffusion constant for heat diffusion. As a result, the MSD of heat diffusion $\langle \Delta x^2(t) \rangle_E$ then depicts at for sufficiently long time t a linear dependence in time t, being the hall mark for normal diffusion.

In summary, normal diffusion for heat is accurately corroborated numerically with the findings depicted with Fig. 1 (c).

$$\left\langle \Delta x^2(t) \right\rangle_E \sim \sum_i i^2 C_E(i,t) = \sum_i i^2 \frac{1}{\sqrt{4\pi D_E t}} e^{-\frac{i^2}{4D_E t}} = 2D_E t \ . \tag{29}$$

Accordingly, heat diffusion theory in [34] for normal diffusion of heat $\langle \Delta x^2(t) \rangle_E$ implies that the heat conduction behavior is normal as well, with the heat conductivity given by $\kappa = c_{\rm V} D_E$.

This Gaussian behavior for $C_E(i,t;j=0,t=0)$ with its corresponding linear time-dependence of the MSD for heat diffusion $\langle \Delta x^2(t) \rangle_E \propto t$ has been observed previously in nonlinear 1D lattices which explicitly do break momentum conservation by including an on-site potential. For example, this is so for the case of 1D lattices with a ϕ^4 on-site potential [35]. In the latter case it is agreed among all practitioners that normal heat conduction occurs beyond any doubt [13, 14]. The situation with momentum-conserving 1D-coupled rotator lattices, however, is far from being settled in the literature [21, 22]. Here the possibility for a diverging thermal conductivity in the thermodynamic limit is still considered as an option by some practitioners. The present state of the art is nonconclusive although prior extensive numerical simulations, using either the Green-Kubo method or the Non-Equilibrium Molecular Dynamics (NEMD) method, both seem to indicate that the thermal conductivity is size-independent [17, 18]. The source of the ongoing dispute is that the numerical results stemming either from the Green-Kubo method and/or the NEMD method, all performed for finite lattice sizes, may possibly not be consistent with manifest asymptotic results in the thermodynamical limit.

In contrast, as we emphasized with the previous section, the energy autocorrelation function $C_E(i,t;j=0,t=0)$ constitutes a fundamental, detailed measure yielding information well beyond the MSD of energy spread $\langle \Delta x^2(t) \rangle_E$ [34, 39]. This is so because of its equivalence with the Green-Kubo formula, which derives from the salient relation detailed with Eq. (5). Put differently, the temporal-spatial distribution of $C_E(i,t;j=0,t=0)$ yields improved, more detailed insight as compared to a method that merely evaluates via MD directly the Green-Kubo integral expression.

Next we study the diffusion of the excess momentum via the momentum autocorrelation function $C_P(i,t;j=0,t=0)$. Our findings are depicted with Fig. 1 (b). One finds that not only does the energy diffusion obey a Gaussian behavior, but also the momentum diffusion occurs Gaussian within our explored large regimes of correlation time spans t.

This behavior of $C_P(i,t;j=0,t=0)$ in this coupled rotator lattice possessing a bounded interaction potential is therefore very distinct from the behavior of the $C_P(i,t;j=0,t=0)$ occurring in the momentum-conserving in FPU-β lattice [35]. Our MSD of the excess momentum $\langle \Delta x^2(t) \rangle_P$ nicely follows a perfect linear time dependence, as can be deduced from Fig. 1 (d).

According to Eq. (24), the viscosity η for this coupled rotator 1D lattice is therefore finite. Put differently, it exhibits a fluidic-like characteristics referred to in the previous section. In distinct contrast, the effective viscosity η for the FPU-β lattice

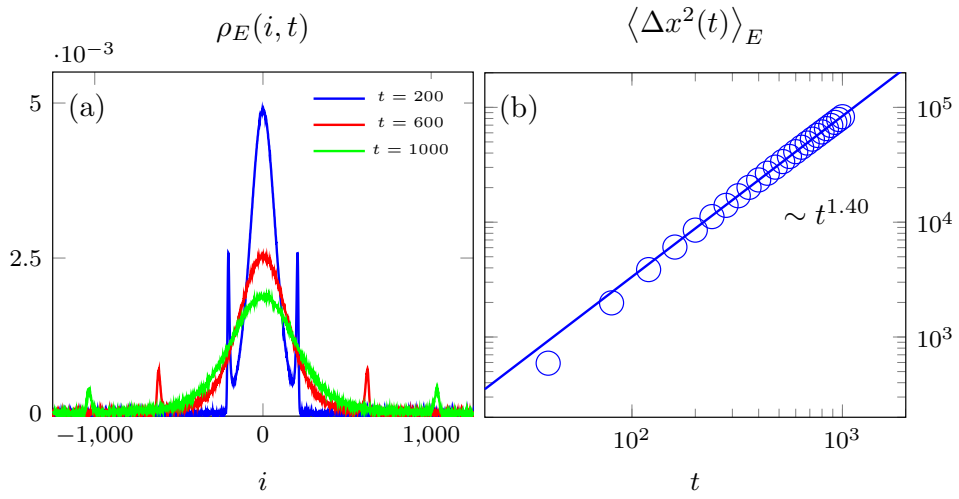

Figure 2. (color online) Heat transport in the amended rotator model with additional harmonic pair interactions: (a): The normalized correlation functions of excess energy density $\rho_E(i,t) = C_E(i,t;j=0,t=0)$ for the rotator with unbounded interaction potentials. The correlation time are $t = 200$ (blue), 600 (red), and 1000 (green). (b): The MSD of the energy spread $\langle \Delta x^2(t) \rangle_E$. The time dependence ceases to be linear for the energy diffusion. The solid blue power law lines serve as a guide to the eye for the power law like behavior of the data in the large time regime. The parameters used in the numerical simulations are $N = 2501$ and $K = 0.5$. The calculated equilibrium temperature is at $T \approx 0.800$.

is diverging towards infinity in the thermodynamic limit; thus displaying the solid-like characteristics, as discussed in section 2, cf. see Eq. (24). In contrast to the case of the FPU-β lattice with three local conservation laws, here the angle $(q_{i+1} - q_i)$ is not conserved. Thus, only two local conservation laws for momentum and energy are present, but none for the stretch (or mass). Nonlinear fluctuating hydrodynamics theory then predicts a central, diffusive spreading for momentum [42] without opposite moving side-peaks; – this being in full agreement with our findings. The investigation of the *momentum* diffusion behavior in this coupled rotator lattice (for a preliminary account see in the arXiv [43]) has inspired renewed attention from other groups as well [44, 45].

4.2. Coupled rotator dynamics amended with harmonic interactions

In testing our hypothesis further we next amend the rotator coupling by adding an additional unbounded, but symmetric harmonic interaction potential. This transforms the original coupled rotator 1D lattice with bounded interaction into a momentum-conserving 1D lattice with a vanishing internal pressure, but now with an unbounded pair interaction, being provided by the harmonic contribution. The Hamiltonian for this so amended coupled rotator model reads:

$$H = \sum_i \left(\frac{p_i^2}{2} + [1 - \cos(q_{i+1} - q_i)] + \frac{K}{2}(q_{i+1} - q_i)^2 \right) , \tag{30}$$

where K denotes the strength of the harmonic interaction. The total momentum is still conserved.

Using the same numerical procedure we numerically study the heat and momentum diffusion for this set up. In Fig. 2 (a), the energy autocorrelation function $C_E(i,t;j=0,t=0)$ at different correlation times is shown. The finite broadened side peaks exhibited by $C_E(i,t;j=0,t=0)$ imply that heat conduction no longer proceeds normal; instead an anomalous, faster–than–linear superdiffusive time dependence of the MSD of the energy spread $\langle \Delta x^2(t) \rangle_E$ is depicted with Fig. 2 (b). This numerically confirms that heat conduction in this unbounded 1D lattice is rendered anomalous. Our numerical fit exhibits this superdiffusive heat spreading, growing as $\langle \Delta x^2(t) \rangle_E \propto t^{1.40}$. Notably, this superdiffusion exponent, $\beta = 1.40$, for the amended rotator model is consistent with a previous result of $\beta = 1.40$ for the FPU-β lattice [35]. Both, the amended rotator model and the FPU-β lattice dynamics dwell a symmetric potential with a corresponding internal vanishing pressure.

We emphasize that the energy autocorrelation function $C_E(i,t;j=0,t=0)$ is directly connected with the transport coefficient of thermal conductivity [34]. In the recent developed *Nonlinear Fluctuation Hydrodynamic Theory* (NFHT) [31, 32], three normal modes, including one central heat mode $f_0(x,t)$ and two opposite moving sound modes $f_{\pm 1}(x,t)$ are obtained upon expanding the three Euler equations up to second order only [32]. Whether such a minimal modification is sufficient to model the transport features is still under debate. In particular, it remains to be shown whether this approximate procedure yields in fact a sufficiently good approximation of the true dynamical transport behavior. In this spirit we hope that our present work sheds more light onto this still open question.

According to Spohn [32], the energy autocorrelation function $C_E(x,t)$ can be decomposed into the three normal modes as $C_E(x,t) = af_{-1}(x,t) + bf_0(x,t) + af_{+1}(x,t)$. The prefactors a and b are model dependent and usually depend on temperature. For example, it is obtained that $a = 0$ and $b = 0.83$ for the FPU-β lattice at $T = 1$ [24]. In this case, the energy autocorrelation function $C_E(x,t)$ and the heat mode $f_0(x,t)$ are equivalent, except for a different value for the prefactor. Therefore, the MSD obtained from the energy autocorrelation function $C_E(x,t)$ and of the central heat mode $f_0(x,t)$ should follow the same time dependence. However, NFHT predicts an exponent of $\beta = 1.50$ for the heat mode in lattices with symmetrical potential at zero pressure [32]. This prediction for $\beta = 1.50$, although quite close, distinctly differs nevertheless from our finding here that $\beta = 1.40$. This value $\beta = 1.40$ agrees, as mentioned above, also with the prior results for the FPU-β lattice dynamics [35, 46].

This discrepancy between the numerical results and the NFHT may originate from an apparent inconsistent assumption employed in Ref. [32]: Namely, in Ref. [32], it is assumed that all the three peaks of the normal modes have a width much less than ct, where c denotes the sound velocity. Using this assumption, one employs the decoupling that the product $f_0(x,t)f_{\pm 1}(x,t) \simeq 0$ for large t. Imposing such zero overlap one proceeds in deriving that the diffusion of the sound modes occurs normal while the

diffusion of heat mode is superdiffusive with an exponent of 1.50. Note however that here the width of the heat mode ($\propto t^{1.50}$) exceeds ct in the asymptotic large time limit, apparently thus contradicting the assumption made.

The question then arises whether this anomalous heat transport behavior is also reflected by the behavior for momentum diffusion. The numerically evaluated momentum autocorrelation function $C_P(i,t;j=0,t=0)$ *vs.* the lattice site is depicted in Fig. 3 (a) for different correlation times. The solely present two side peaks move outwards with a constant sound velocity c, giving rise to a ballistic diffusion behavior for the momentum autocorrelation function $C_P(i,t;j=0,t=0)$ with the leading term proportional to c^2t^2. The true diffusion behavior of momentum is reflected by the subleading term or the self-diffusion of the side peaks themselves [42]. The best way to illustrate this momentum behavior of self-diffusion is to present the decay of the height of the side peaks as a function of time. For a normal diffusion behavior this decay of the height of the peaks must follow an inverse square root law, being proportional to $t^{-0.5}$. A decay faster than $t^{-0.50}$ does manifest itself as a non-diffusive, superdiffusive behavior. Indeed this feature is corroborated numerically with a behavior for the decay of the central height of the peak(s) of $C_P(i,t;j=0,t=0)$, which is found to be proportional to $t^{-0.55}$. This can be detected clearly from Fig. 3 (b). In order to double-check this non-diffusive behavior of the momentum self-diffusion, we plot the rescaled side peaks of $C_P(i,t;j=0,t=0)\cdot t^{\gamma}$ in a co-moving frame at the sound velocity c for different times: in Fig. 3 (c) with $\gamma=0.50$ (diffusive) and in (d) with $\gamma=0.55$ (non-diffusive). It is fair to say that the value $\gamma=0.55$ fits much better the data. This in turn indicates that the self-diffusion behavior of the momentum is non-diffusive for the symmetrically amended rotator model at zero pressure. For this model, the momentum autocorrelation function $C_P(i,t;j=0,t=0)$ coincides with the two sound normal modes $f_{\pm1}$ defined in NFHT. However, our numerical results of $\gamma=0.55$ again deviates from the prediction that $\gamma=0.50$ from NFHT [32].

4.3. Hard point gas model with a square well potential and alternating masses

The hard point gas model mimics a sort of idealized fluid with unbounded interactions strength. The Hamiltonian of a one-dimensional hard point gas model can be expressed as [33]:

$$H_{HPG}=\sum_{i=1}^{N}\frac{1}{2m_i}p_i^2+\frac{1}{2}\sum_{i\neq j=1}^{N}V(q_i-q_j)\ , \tag{31}$$

where the setup of masses $m_i=1$ for even i and $m_i=3$ for odd i, see in Ref. [33]. This choice converts this model into a non-integrable dynamics with strong mixing properties. The latter aspect is advantageous when it comes to the convergence issues at long times and large sizes in MD simulations. The symmetric square-well interaction potential reads [33]

$$V_{sw}(x)=0,\ \text{if}\ 0<|x|<1;\ \ V_{sw}(x)=\infty,\ \text{otherwise}\ . \tag{32}$$

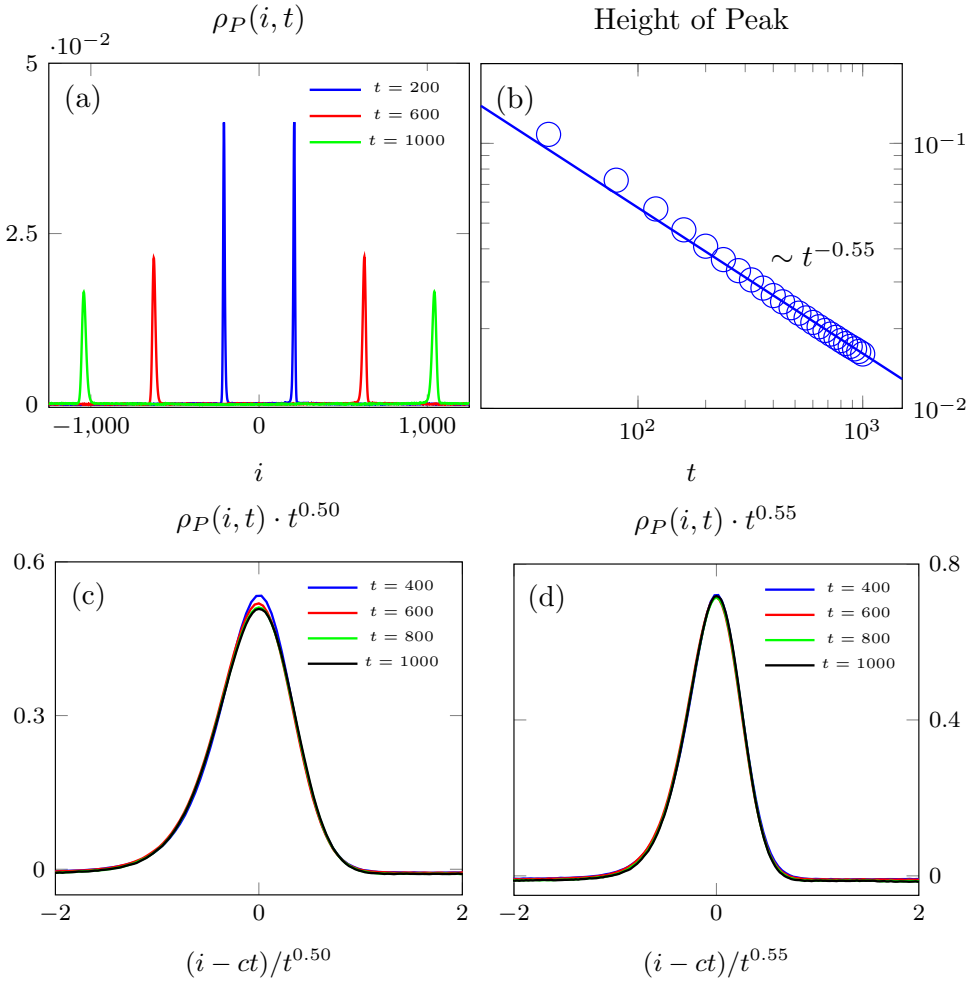

Figure 3. (color online) Excess momentum spread in the amended coupled rotator model with additional harmonic pair interactions present: (a): The normalized correlation functions of excess momentum density $\rho_P(i,t) = C_P(i,t;j=0,t=0)$ for the rotator with unbounded interaction potentials. The correlation time are $t = 200$ (blue), 600 (red), and 1000 (green). Each has two symmetric side peaks moving outside with a constant sound velocity c. (b): The decay of the height of the side peak of $\rho_P(i,t)$. The solid blue power law lines with the dependence of $\sim t^{-0.55}$ is the best fit for the data from $t = 400$ to $t = 1000$. (c) The rescaled plot of the side peaks of $\rho_P(i,t)$ with the exponent of 0.50 in the moving frame of sound velocity c at $t = 400, 600, 800$ and 1000. (d) The rescaled plot of the side peaks of $\rho_P(i,t)$ with the exponent of 0.55 in the moving frame of sound velocity c at $t = 400, 600, 800$ and 1000. The parameters used in the numerical simulations are $N = 2501$ and $K = 0.5$. The calculated equilibrium temperature is at $T \approx 0.800$.

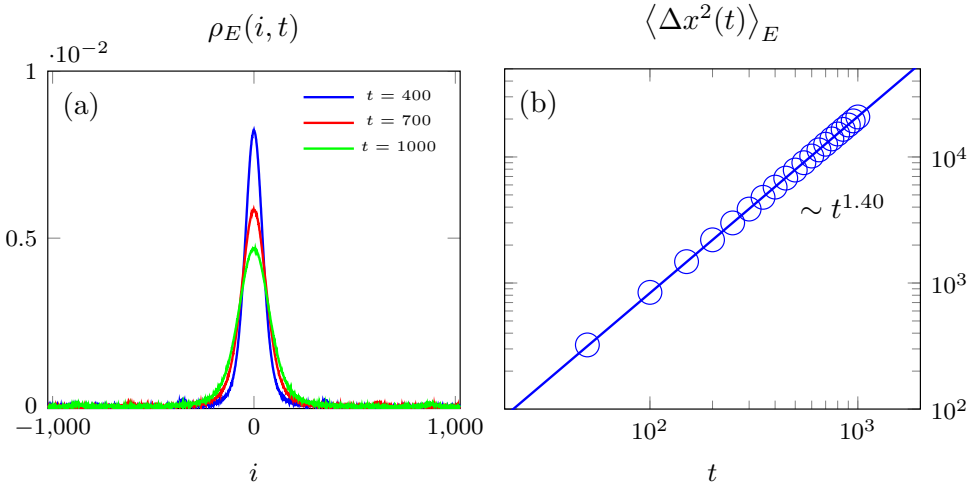

Figure 4. (color online) Spreading of heat in the hard point gas model with symmetric square-well interaction potential with alternating masses at zero internal pressure: (a): The normalized energy correlation functions of excess energy density $\rho_E(i,t) = C_E(i,t;j=0,t=0)$. The correlation times are $t = 400$ (blue), 700 (red), and 1000 (green). (b): The anomalous MSD of the energy spread $\langle \Delta x^2(t) \rangle_E$. The solid blue power law lines serve as a guide to the eye for the power law like behavior of the data in the asymptotic large time regime. The parameters used in the numerical simulations are identical to the choice made in Ref. [33] with a total number of particles $N = 4096$.

Because each unit cell contains two particles, the local energy H_j and the momentum p_j used for calculation need to be redefined as $H_j = H_{2j-1} + H_{2j}$ and the local momentum as $p_j = p_{2j-1} + p_{2j}$ where the number of unit cells amounts to half of the total particles.

According to NFHT [32], this hard point gas model with a square well interaction potential and alternating masses can be classified into the same class as the FPU-β lattice, and alike the amended coupled rotator model. In this model, the energy and momentum autocorrelation functions $C_E(i,t;j=0,t=0)$ and $C_P(i,t;j=0,t=0)$ coincide with the heat mode f_0 and sound modes $f_{\pm 1}$ in the NFHT, respectively. The NFHT predicts that the energy diffusion is Levy walk superdiffusive with $\langle \Delta x^2(t) \rangle_E \propto t^{1.50}$, whereas the self-diffusion of momentum is predicted within NFHT to be normal diffusive.

In Fig. 4 (a), we depict the energy autocorrelation function $C_E(i,t;j=0,t=0)$ at different times. Compared with the amended rotator model and the FPU-β lattice, the two side peaks are much smaller, although still not vanishing (being only barely visible in Fig. 4 (a)). The MSD of the energy spread is plotted in Fig. 4 (b), yielding a superdiffusive behavior with $\langle \Delta x^2(t) \rangle_E \propto t^{1.40}$. As for the FPU-$\beta$ lattice and our amended coupled rotator model result our finding distinctly deviates from the NFHT prediction; it is however consistent with our numerical results of amended rotator model as well as the previously studied FPU-β lattice, which all yield numerically an exponent $\beta = 1,40$. This again may indicate that NFH-Theory is quite good, although not

sufficiently accurate enough to account for the full nonlinear dynamics at work.

Of greater concern are the deviations for momentum spread which theory predicts to be normal but which seemingly does not fit our numerical results. The momentum autocorrelation functions $C_P(i,t;j=0,t=0)$ at different times are depicted in Fig. 5 (a). Here we find results that are quite similar to the amended coupled rotator model: The two side sound peaks move in opposite direction with a constant sound speed c. To explore the momentum self-diffusion behavior in greater detail, we closely investigate the decay of the central height of the two side peaks, see in Fig. 5 (b). This decay of the height of the peak are best fitted with a decay law proportional to $t^{-0.57}$. Being different from the normal diffusive scaling $t^{-0.5}$ this indicates a non-diffusive behavior for the momentum spread. The rescaled momentum excess density $C_P(i,t;j=0,t=0)\cdot t^{\gamma}$ in the co-moving frame of the sound velocity of the center of the side peaks are plotted in Fig. 5 (c) with (i) $\gamma = 0.50$ (normal diffusion) and also (d) with (ii) $\gamma = 0.57$ (anomalous superdiffusion). Most importantly, the curves with $\gamma = 0.57$ fit convincingly better with the numerical data. This feature therefore reconfirms (contrary to the NFHT prediction [32, 33]) anomalous momentum spread for the hard point gas with a square well interaction potential.

4.4. Testing a Lennard-Jones pair interaction

Inspecting the preceding three test model cases one is led to speculate that it may well be the unbounded part of the interaction potential that is at the cause for a normal heat and momentum transport behavior in nonlinear 1D momentum-conserving lattices. Such a reasoning has obtained support in view of the recent numerical studies by Savin and Kosevich [23] which numerically find that heat conductivity remains finite in 1D interaction potentials possessing a regime that allows for dissociation at asymptotic large interaction distances as it occurs, for example, with the Lennard-Jones 1D case. If so, then for our hypothesis to hold up we should find that in this case the subleading momentum self-diffusion behavior should emerge normal.

Using the same numerical schemes as for the foregoing three lattice cases we next test our hypothesis for a Lennard-Jones setup. The corresponding Hamiltonian is given by

$$H = \sum_i \left[\frac{p_i^2}{2} + 4\varepsilon \left((\frac{\sigma}{1+q_{i+1}-q_i})^6 - \frac{1}{2} \right)^2 \right], \tag{33}$$

using the same parameters as in Savin and Kosevich's paper; i.e., $\sigma = 2^{-1/6}$ and a binding energy $\varepsilon = 1/72$ [23]. Here, the pair interaction potential is unbounded at short interaction distances but becomes free at large interaction distances, allowing dissociation. Due to this asymmetry in the interaction potential the internal pressure Λ assumes a finite value. The autocorrelation functions $C_E(i,t;j=0,t=0)$ and $C_P(i,t;j=0,t=0)$ for energy and momentum are defined as before with Eqs. (2) and (10), respectively.

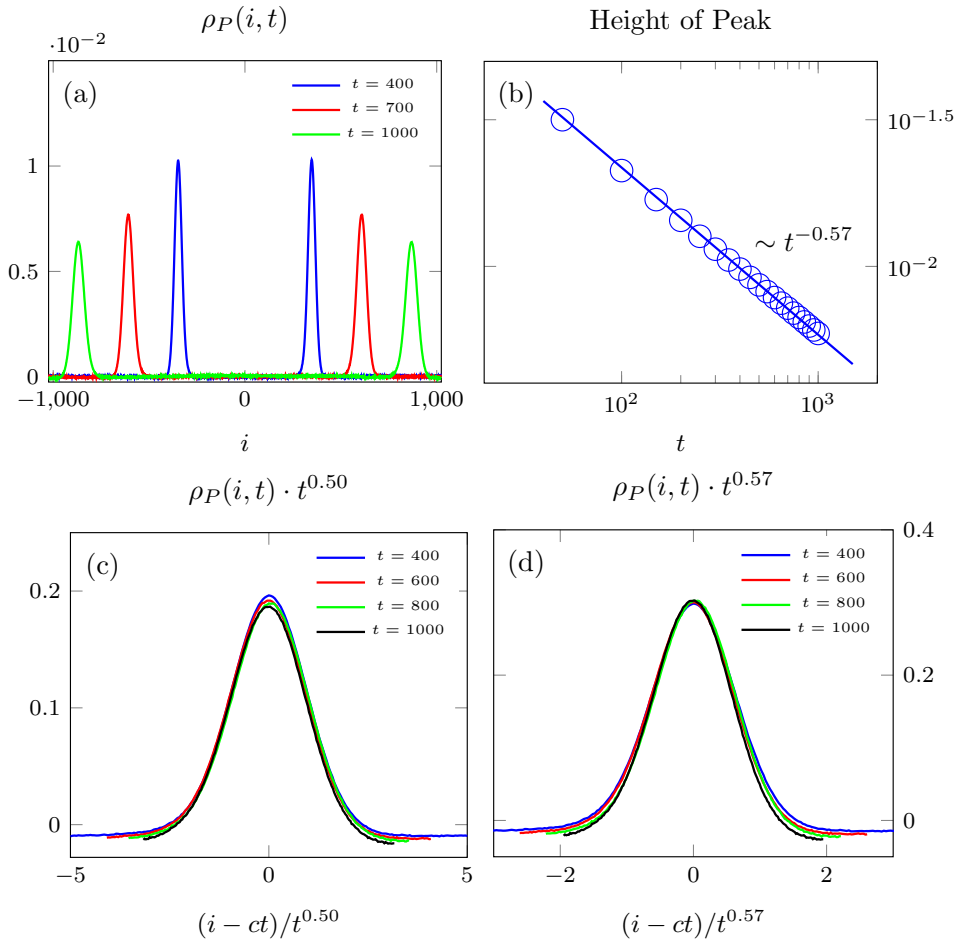

Figure 5. Momentum spread in the hard point gas model with a square-well interaction potential composed of alternating masses at vanishing internal pressure: (a): The normalized correlation functions of excess momentum density $\rho_P(i,t) = C_P(i,t;j=0,t=0)$. The correlation times are $t = 400$ (blue), 700 (red), and 1000 (green). Each has two symmetric side peaks moving in opposite direction with a constant sound velocity c. (b): The decay of the height of the side peaks of $\rho_P(i,t)$. The solid blue power law lines depict a decay law proportional to $\sim t^{-0.57}$ as the best fit for the data from $t = 400$ to $t = 1000$. (c) The rescaled plot of the side peaks of $\rho_P(i,t)$ with the exponent 0.50 in the co-moving frame of the sound speed c at $t = 400, 600, 800$ and 1000. (d) The rescaled plot of the side peaks of $\rho_P(i,t)$ with the exponent of 0.57 in the moving frame of sound velocity c at $t = 400, 600, 800$ and 1000. The parameters used in the numerical simulations are the same as in Ref. [33] with $N = 4096$.

In Fig. 6 (a), we depict the correlation functions $C_E(i,t;j=0,t=0)$ for the energy diffusion versus the correlation time t. For sufficient large times t we observe that the energy autocorrelation function $C_E(i,t;j=0,t=0)$ evolves with two broadened side peaks, being rather distinct from a normal, Gaussian-like energy distribution spreading. Consequently, the corresponding energy MSD is therefore not normal, i.e. it is not proportional to time t. In fact it assumes at long times a power-law like behavior, being below an overall ballistic spreading, cf. Fig. 6 (b).

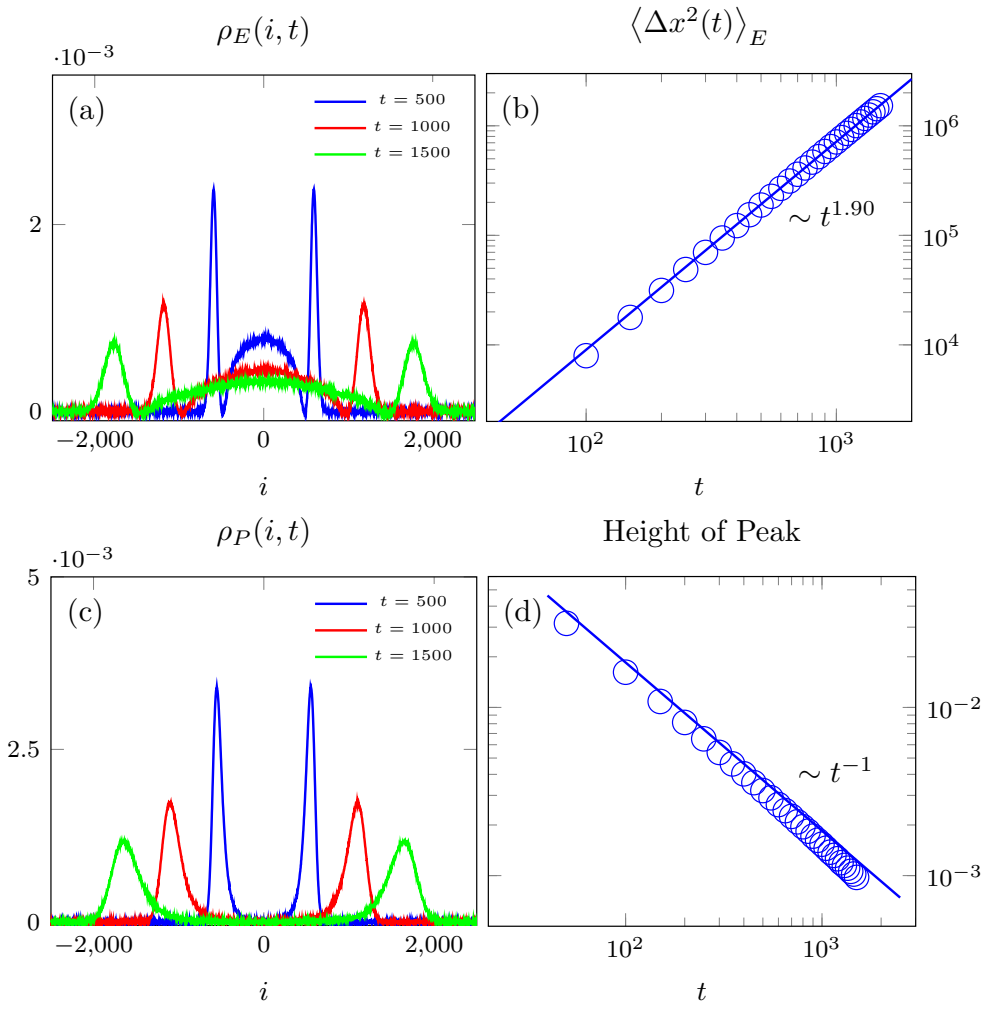

Figure 6. (color online) Energy spread in a 1D Lennard-Jones lattice system. (a) and (c): The normalized correlation functions of the excess energy density and excess momentum density $\rho_E(i,t) = C_E(i,t;j=0,t=0)$, $\rho_P(i,t) = C_P(i,t;j=0,t=0)$ for the case with a Lennard-Jones interaction potential. The correlation times are $t = 500$ (blue),1000 (red), and 1500 (green). (b): The MSD of the energy spread $\langle \Delta x^2(t) \rangle_E$. (d): The decay of the height of the side peaks of $\rho_P(i,t)$. In both situations (b) and (d), the solid blue power law lines serve as a guide to the eye for the data in the large time regime. The parameters in the numerical simulations are for $N = 5001$, $\sigma = 2^{-1/6}$ and $\varepsilon = 1/72$, which are the same parameters as used in Savin and Kosevich's paper [23]. The calculated equilibrium temperature is at $T \approx 0.002$.

Let us next also study the momentum spread for this test case. In Fig. 6 (c), the momentum autocorrelation function $C_P(i,t;j=0,t=0)$ at different times are shown. The decay of the height of the side peaks are also depicted with Fig. 6 (d). We detect numerically a behavior for the decay of the peak heights proportional to t^{-1}. In perfect agreement with our stated hypothesis, we thus find as well a non-diffusive momentum self-diffusion for this forth test case. Our findings not only contradict the recent results reported with [23], predicting therein a normal behavior for heat transport, but as well make evident that it is *not* necessarily the shape of the interaction potential which rules

whether transport proceeds normal or anomalous.

5. Conclusions and outlook

The objective of studying energy and momentum transport in low-dimensional systems has recently attracted renewed interest in view of profound advances in theory, namely (i) the derivation of new transport relations [34] and (ii) new insight into scaling behaviors [24, 31, 32, 33, 36]. Apart from the role of energy spread and energy transport also the problem of associated momentum spread and momentum transport gained recent attention [32, 35, 43, 44]. Despite this recent progress many open problems remain and the regime of validity of approximate theory predictions, most prominently for the appealing nonlinear fluctuating hydrodynamics theory [32], is still under active debate.

With this work we studied transport and diffusion characteristics of different classes of momentum-conserving nonlinear $1D$ Hamiltonian dynamics for both, heat and momentum. Using recent results of Ref. [34] we started out showing that for energy diffusion there exists a close relationship between the behavior of excess energy diffusion and the overall conductivity behavior for thermal heat transport. This relationship has then been generalized alike for the case of momentum diffusion in 1D nonlinear lattices. For the subleading part of momentum spread beyond its possible ballistic transport yields a diffusivity which relates to the time derivative of the asymptotic MSD for excess momentum, see in Eq. (25). The consideration of momentum spread offers the possibility to quantify an effective viscosity, being proportional to the momentum diffusivity, Eq. (26). For normal momentum diffusion this effective viscosity is finite while it diverges with increasing time t if the intrinsic momentum diffusion occurs superdiffusive.

A main open problem in this field is the question when and under what conditions the energy and momentum transport deviate from normal. Put differently, when is transport and diffusive spreading occurring anomalously in low dimensional nonlinear Hamiltonian systems. – In this context the authors here put forward their speculative hypothesis that normal (anomalous) heat transport has its origin in normal (anomalous) momentum spread, and vice versa. Having no proof available for this hypothesis we tested the claim by investigating numerically four different nonlinear model systems of momentum conserving nonlinear dynamics that are expected to belong to different classes for their energy/momentum transport characteristics. These were (i) the coupled rotator dynamics, (ii) its generalization involving the addition of unbounded harmonic interactions, (iii) the hard point gas and (iv) a case with an asymptotic free dissociation regime (Lennard-Jones interaction potential).

As a main finding from these extensive numerical simulations we can assess that our so stated hypothesis does hold up. This encouraging positive result, however, does not assure that it is fundamentally correct, as we have tested only a finite sample of nonlinear Hamiltonian models. Moreover, one may argue fairly that any numerical

verification lacks a profound analytical foundation. Particularly, the question remains whether the numerical findings still hold true in the extreme asymptotic regime of time $t \to \infty$, being beyond any numerical accessibility at this time. It can be convincingly stated, however, that the mere conservation of momentum in 1D Hamiltonian systems does generally not imply anomalous transport.

Our simulations also shed new light on the question of whether the recent NFHT [32] is accurate enough to predict the scaling regimes for energy and momentum transport. As mentioned, this theory is approximative in that it is based on a expansion of the Euler equations to second order only. In addition, it involves further approximations such as a decoupling of different modes at large times, which seemingly cannot be convincingly justified in presence of anomalous, superdiffusive energy transport. Nevertheless, this theory admittedly is the best available at present times. Its scaling prediction for energy transport in models with symmetric unbounded interaction potentials yields an exponent $\beta = 0.50$; this being quite close, but still distinctly different from our numerical value that $\beta = 0.40$. Even more interesting is the prediction of NFHT that momentum spread should occur normal in these cases, thus violating our stated hypothesis. Our precise numerics shows however that such a normal momentum diffusion behavior does not fit with our numerical findings. This has been shown with the non-diffusive decay characteristics of the central peaks of the two opposite moving two side peaks in the excess momentum density function. This deviation is additionally substantiated with the failure of a collapse of the data for an assumed normal diffusion in the co-moving frame of sound propagation. The behavior rather fits beautifully, however, with a collapse using *anomalous* momentum diffusion; – thereby corroborating our stated hypothesis. In this context we may point out that similar deviations from a normal diffusive scaling for the sound mode are present in the numerics performed by the advocates of NFHT: upon inspecting Fig. 8 in Ref. [24] one detects a similar failure of a diffusive collapse. The numerically established failure here of a diffusive collapse for the case of the fully chaotic hard point gas is particularly trustworthy as we profit from underlying fast numerical converge features.

An interesting question for future studies is whether the criterion can be extended to anomalous/normal heat flow occurring in two-dimensional momentum-conserving nonlinear lattice systems. Typically, the anomalous heat conductance then tends to diverge in system size logarithmically [1, 2, 11, 47, 48, 49, 50]. Last but not least, the discussed complexity of normal versus anomalous heat and momentum transport in low dimensions might possibly be put to constructive use when designing 1D low dimensional devices for function, such as it is the case for the timely topic of "phononics" [51].

6. Acknowledgements

The authors much appreciate those many mutually stimulating and insightful correspondences with Professor Herbert Spohn. We also appreciate the useful correspondence with Professor Abhishek Dhar and his collaborators. The numerical

calculations were carried out at Shanghai Supercomputer Center, which has been supported by the NSF China with grant No. 11334007 (B.L.). This work has been supported by the NSF China with grant No. 11334007 (Y.L., N.L., B.L.), the NSF China with Grant No. 11205114 (N.L.), the Program for New Century Excellent Talents of the Ministry of Education of China with Grant No. NCET-12-0409 (N.L.), the Shanghai Rising-Star Program with grant No. 13QA1403600 (N.L.), the NSF China with grant No. 11347216 (Y.L.) and Tongji University grant No. 2013kJ025 (Y.L.).

7. Appendix

7.1. Dimensionless units

For the investigation of the dynamics of 1D nonlinear lattice models, dimensionless units have been applied throughout as a convenient tool. As discussed in Ref. [51], the setup of dimensionless units is model dependent. We will elaborate below the details of the used dimensionless units for the 1D nonlinear lattice models considered in this work.

7.1.1. Coupled rotator model. The dimensional Hamiltonian of coupled rotator model can be expressed as

$$H = \sum_i \left(\frac{p_i^2}{2m} + V \left[1 - \cos \frac{2\pi(q_{i+1} - q_i)}{a} \right] \right) , \tag{34}$$

where p_i and q_i denote the dimensional momentum and displacement from equilibrium position for i-th atom. m denotes the atom mass and a is the lattice constant. The parameter V, possing the dimension of energy, represents the coupling strength of the neighboring rotators.

For this coupled rotator model, one can introduce the dimensionless variables by measuring lengths in units of $[a/(2\pi)]$, energies in units of $[V]$, masses in units of $[m]$, momenta in units of $[(Vm)^{1/2}]$, time in units of $[am^{1/2}/(2\pi V^{1/2})]$. The temperature will be measured in units of $[V/k_B]$ where k_B is the Boltzmann constant. If we implement the following substitutions:

$$H \to H[V],\ p_i \to p_i[(Vm)^{1/2}],\ q_i \to q_i[a/(2\pi)] . \tag{35}$$

The Hamiltonian of Eq. (34) can be transformed into the dimensionless one of Eq. (27).

7.1.2. Amended coupled rotator model. The dimensional Hamiltonian of amended rotator model is

$$H = \sum_i \left(\frac{p_i^2}{2m} + V \left[1 - \cos \frac{2\pi(q_{i+1} - q_i)}{a} \right] + \frac{k_0}{2}(q_{i+1} - q_i)^2 \right) , \tag{36}$$

where k_0 denotes the extra coupling strength between neighboring atoms. The dimensionless units setup is the same as that for coupled rotator model. Applying the same transformation of Eq. (35), Eq. (36) can be transformed into the dimensionless Hamiltonian of Eq. (30) with the dimensionless $K = a^2 k_0/(4\pi^2 V)$.

7.1.3. Hard point gas with alternating masses with square well potential. The dimensional Hamiltonian of hard point gas model is

$$H = \sum_{i}^{N} \frac{p_i^2}{2m_i} + \frac{1}{2} \sum_{i \neq j=1}^{N} V(q_i - q_j) \ , \tag{37}$$

where m_i is the mass for i-th particle and the square well potential can be described as

$$V_{sw}(x) = 0, \text{ if } 0 < |x| < a; \ \ V_{sw}(x) = \infty, \text{ otherwise} \ , \tag{38}$$

with a denoting the average distance between neighboring particles. The alternating masses are introduced by setting particle masses $m_i = m_0$ for an even number of i and $m_i = 3m_0$ for an odd number of i.

For this hard point gas model, one can introduce the dimensionless variables by measuring lengths in units of $[a]$, masses in units of $[m_0]$. Since there is no characteristic potential energy for this model, its dynamics is essentially the same for any energy scale. One can arbitrarily choose an energy scale E_0 as the reference energy and the energies can be measured in units of $[E_0]$. As a result, the momenta can be measured in units of $[(m_0 E_0)^{1/2}]$ and the time can be measured in units of $[a(m_0/E_0)^{1/2}]$. The temperature can also be measured in units of $[E_0/k_B]$. In our study we used the same parameters as used in Ref. [33].

7.1.4. Lennard-Jones model. The dimensional Lennard-Jones model has the following Hamiltonian

$$H = \sum_{i} \left[\frac{p_i^2}{2m} + 4\varepsilon\varepsilon_0 \left(\left(\frac{\sigma}{1 + (q_{i+1} - q_i)/a} \right)^6 - \frac{1}{2} \right)^2 \right] \ , \tag{39}$$

where m is the atom mass and a is the lattice constant. $\varepsilon\varepsilon_0$ denotes the binding energy and ε is a dimensionless parameter. σ is yet another dimensionless parameter.

For this Lennard-Jones model, one can introduce the dimensionless variables by measuring lengths in units of $[a]$, masses in units of $[m]$, energies in units of $[\varepsilon_0]$, momenta in units of $[(\varepsilon_0 m)^{1/2}]$, time in units of $[a(m/\varepsilon_0)^{1/2}]$. The temperature will be measured in units of $[\varepsilon_0/k_B]$. If we implement the following substitutions

$$H \to H[\varepsilon_0], \ p_i \to p_i[(\varepsilon_0 m)^{1/2}], \ q_i \to q_i[a] \ . \tag{40}$$

The Hamiltonian of Eq. (39) can then be transformed into the dimensionless Hamiltonian of Eq. (33).

7.2. Numerical procedures

In order to obtain precise numerical results, we employ MD simulations for an isolated system evolving with the corresponding Liouvillian over large, extended time spans and used throughout periodic boundary conditions. The method to obtain the correlation functions is adopted from Ref. [52]. The equations of motions are integrated with a fourth order symplectic algorithm [53, 54].

References

[1] Lepri S, Livi R, and Politi A 2003 *Phys. Rep.* **377** 1
[2] Dhar A 2008 *Adv. Phys.* **57** 457
[3] Liu S, Xu X F, Xie R G, Zhang G and Li B 2013 *Eur. Phys. J. B* **85** 337
[4] Kaburaki H and Machida M 1993 *Phys. Lett. A* **181** 85
[5] Lepri S, Livi R and Politi A 1997 *Phys. Rev. Lett.* **78** 1896
[6] Hatano T 1999 *Phys. Rev. E* **59** 1(R)
[7] Zhang G and Li B 2005 *J. Chem. Phys.* **123** 114714
[8] Yang N, Zhang G, and Li B 2010 *Nano Today* **5** 85
[9] Liu J and Yang R 2012 *Phys. Rev. B* **86**, 104307
[10] Chang C W, Okawa D, Garcis H, Majumdar A and Zettl A 2008 *Phys. Rev. Lett.* **101** 075903
[11] Xu X, Pereira L, Wang Y, Wu J, Zhang K, Zhao X, Bae S, Hui C T, Xie R, Thong J T L, Hong B H, Loh K P, Donadio D, Li B and Özyilmaz B 2014 *Nat. Commun.* **5** 3689
[12] Hu B, Li B and Zhao H 1998 *Phys. Rev. E* **57** 2992
[13] Hu B, Li B and Zhao H 2000 *Phys. Rev. E* **61** 3882
[14] Aoki K and Kusnezov D 2000 *Phys. Lett. A* **265** 250
[15] Prosen T and Campbell D K 2000 *Phys. Rev. Lett.* **84** 2857
[16] Narayan O and Ramaswamy S 2002 *Phys. Rev. Lett.* **89** 200601
[17] Giardinà C, Livi R, Politi A and Vassalli M 2000 *Phys. Rev. Lett.* **84** 2144
[18] Gendelman O and Savin A 2000 *Phys. Rev. Lett.* **84** 2381
[19] Lee-Dadswell G R, Turner E, Ettinger J and Moy M 2010 *Phys. Rev. E* **82** 061118
[20] Giardinà C and Kurchan J 2005 *J. Stat. Mech.* **5** P05009
[21] Flach S, Miroshnichenko A E and Fistul M V 2003 *Chaos* **13** 596
[22] Li B, Wang J, Wang L and Zhang G 2005 *Chaos* **15** 015121
[23] Savin A V and Kosevich Y A, 2014 *Phys. Rev. E* **89** 032102
[24] Das S G, Dhar A, Saito K, Mendl C B and Spohn H 2014 *Phys. Rev. E* **90** 012124
[25] Helfand E 1960 *Phys. Rev.* **119** 1
[26] Denisov S, Klafter J and Urbakh M 2003 *Phys. Rev. Lett.* **91** 194301
[27] Zaburdaev V, Denisov S and Hänggi P 2011 *Phys. Rev. Lett.* **106** 180601
[28] Zaburdaev V, Denisov S and Hänggi P 2011 *Phys. Rev. Lett.***109** 069903
[29] Dhar A, Saito K and Derrida B 2013 *Phys. Rev. E* **87** 010103
[30] van Beijeren H 2012 *Phys. Rev. Lett.* **108** 180601
[31] Mendl C B and Spohn H 2013 *Phys. Rev. Lett.* **111** 230601
[32] Spohn H 2014 *J. Stat. Phys.* **154** 1191
[33] Mendl C B and Spohn H 2014 *Phys. Rev. E* **90** 012147
[34] Liu S, Hänggi P, Li N, Ren J and Li B 2014 *Phys. Rev. Lett.* **112** 040601
[35] Zhao H 2006 *Phys. Rev. Lett.* **96** 140602
[36] Liu S, Liu J, Hänggi P, Wu C and Li B 2014 *Phys. Rev. B* **90** 174304
[37] Visscher W M 1974 *Phys. Rev. A* **10** 2461
[38] Allen P B and Feldman J L 1993 *Phys. Rev. B* **48** 12581
[39] Li N, Li B and Flach S 2010 *Phys. Rev. Lett.* **105** 054102
[40] Hänggi P and Thomas H 1982 *Phys. Rep.* **88** 207
[41] Resibois P. and de Leener M. *Classical Kinetic Theory of Fluids* (John Wiley and Sons, New York, London, Sidney, Toronto, 1977)
[42] Spohn H 2014 *private communication*
[43] Li Y, Liu S, Li N, Hänggi P and Li B, arXiv:1407.1161v1
[44] H. Spohn, arXiv:1411.3907v1
[45] Das S and Dhar A, arXiv:1411.5247v2
[46] Wang L and Wang T 2011 *EPL* **93** 54002
[47] Lippi A and Livi R 2000 *J. Stat. Phys.* **100** 1147

[48] Yang L, Grassberger P and Hu B 2006 *Phys. Rev. E* **74** 062101
[49] Xiong D, Wang J, Zhang Y and Zhao H 2010 *Phys. Rev. E* **82** 030101
[50] Wang L, Hu B and Li B 2012 *Phys. Rev. E* **86** 040101(R)
[51] Li N, Ren J, Wang L, Zhang G, Hänggi P and Li B 2012 *Rev. Mod. Phys.* **84** 1045
[52] Chen S, Zhang Y, Wang J and Zhao H 2013 *Phys. Rev. E* **87** 032153
[53] Laskar J and Robutel P 2001 *Celest. Mech. Dyn. Astron.* **80** 39
[54] Skokos Ch, Krimer D O, Lomineas S and Flach S 2009 *Phys. Rev. E* **79** 056211